LETTER

doi:10.1038/nature20810

Pathologically expanded peripheral T helper cell subset drives B cells in rheumatoid arthritis

Deepak A. Rao[1], Michael F. Gurish[1], Jennifer L. Marshall[2], Kamil Slowikowski[1,3,4,5,6], Chamith Y. Fonseka[1,3,4,6,7], Yanyan Liu[1], Laura T. Donlin[8,9], Lauren A. Henderson[10], Kevin Wei[1], Fumitaka Mizoguchi[1], Nikola C. Teslovich[1,3,4], Michael E. Weinblatt[1], Elena M. Massarotti[1], Jonathan S. Coblyn[1], Simon M. Helfgott[1], Yvonne C. Lee[1], Derrick J. Todd[1], Vivian P. Bykerk[11,12], Susan M. Goodman[11,12], Alessandra B. Pernis[9,12,13], Lionel B. Ivashkiv[8,9], Elizabeth W. Karlson[1], Peter A. Nigrovic[1,10], Andrew Filer[2], Christopher D. Buckley[2], James A. Lederer[14], Soumya Raychaudhuri[1,3,4,5,15,16] & Michael B. Brenner[1]

CD4$^+$ T cells are central mediators of autoimmune pathology; however, defining their key effector functions in specific autoimmune diseases remains challenging. Pathogenic CD4$^+$ T cells within affected tissues may be identified by expression of markers of recent activation[1]. Here we use mass cytometry to analyse activated T cells in joint tissue from patients with rheumatoid arthritis, a chronic immune-mediated arthritis that affects up to 1% of the population[2]. This approach revealed a markedly expanded population of PD-1^{hi}CXCR5$^-$CD4$^+$ T cells in synovium of patients with rheumatoid arthritis. However, these cells are not exhausted, despite high PD-1 expression. Rather, using multidimensional cytometry, transcriptomics, and functional assays, we define a population of PD-1^{hi}CXCR5$^-$ 'peripheral helper' T (T_{PH}) cells that express factors enabling B-cell help, including IL-21, CXCL13, ICOS, and MAF. Like PD-1^{hi}CXCR5$^+$ T follicular helper cells, T_{PH} cells induce plasma cell differentiation *in vitro* through IL-21 secretion and SLAMF5 interaction (refs 3, 4). However, global transcriptomics highlight differences between T_{PH} cells and T follicular helper cells, including altered expression of BCL6 and BLIMP1 and unique expression of chemokine receptors that direct migration to inflamed sites, such as CCR2, CX3CR1, and CCR5, in T_{PH} cells. T_{PH} cells appear to be uniquely poised to promote B-cell responses and antibody production within pathologically inflamed non-lymphoid tissues.

We analysed CD4$^+$ T cells in three seropositive (defined as positive for rheumatoid factor or anti-citrullinated-peptide antibody) rheumatoid arthritis (RA) synovial tissue samples with dense leukocyte infiltrates, using a mass cytometry panel designed to interrogate both stromal and leukocyte populations (Extended Data Table 1). Two-dimensional visualization of the multidimensional cytometry data using viSNE (visualization using t-Distributed Stochastic Neighbor Embedding)[5] revealed a heterogeneous CD4$^+$ T-cell population with distinct expression patterns of five activation markers (PD-1, MHC II, ICOS, CD69, and CD38) (Fig. 1a). Notably, a large population of cells with high PD-1 expression clustered together in each of the three samples (Fig. 1a, Extended Data Fig. 1a). Biaxial gating of data from six seropositive RA synovial tissue samples confirmed high expression of PD-1 on ~25% of synovial CD4$^+$ T cells, the majority of which co-expressed MHC II and/or ICOS (Fig. 1b, Extended Data Fig. 1b, Extended Data Table 2).

In a complementary approach, 11-dimensional flow cytometric analysis of memory CD4$^+$ T cells from paired synovial fluid and blood samples from three seropositive RA patients also revealed a large population of synovial PD-1^{hi}CD4$^+$ T cells, a subset of which co-expressed MHC II and/or ICOS (Extended Data Fig. 1c). Approximately 30% of synovial fluid CD4$^+$ T cells displayed high PD-1 expression, mirroring results from synovial tissue (Fig. 1c, Extended Data Fig. 1c, d). The frequency of PD-1^{hi}CD4$^+$ T-cell populations was over fivefold higher in seropositive RA synovial fluid ($n = 9$) compared to synovial fluid from 19 patients with seronegative inflammatory arthritides (seronegative RA $n = 2$, spondyloarthropathy $n = 8$, juvenile idiopathic arthritis $n = 9$) (Fig. 1c).

The marked expansion of PD-1^{hi} cells specifically in seropositive RA, a disease characterized by autoantibody production and frequent synovial T–B-cell aggregates[6,7], led us to consider whether synovial PD-1^{hi} cells might be T follicular helper (T_{FH}) cells. T_{FH} cells, often identified as CXCR5$^+$ PD-1$^+$, are uniquely adapted to promote B-cell recruitment and differentiation in lymph node follicles through production of IL-21, IL-4, CD40L, and CXCL13, the ligand for CXCR5 (ref. 3). However, seropositive RA synovial tissue samples contained few PD-1^{hi}CXCR5$^+$ T_{FH} cells (Fig. 1d), which clustered separately from PD-1^{hi}CXCR5$^-$ cells in viSNE analyses (Fig. 1a). By contrast, ~85% of PD-1^{hi}CD4$^+$ cells in synovial tissue lacked CXCR5, as did almost all PD-1^{hi}CD4$^+$ cells in synovial fluid (Fig. 1d). Measurement of *CXCR5* transcript levels in sorted PD-1^{hi}CXCR5$^-$ and PD-1^{hi}CXCR5$^+$ cells from synovial tissue, synovial fluid, and blood confirmed that PD-1^{hi}CXCR5$^-$ cells from all three sources contained little, if any, *CXCR5* mRNA (Extended Data Fig. 1e, f). Thus, seropositive RA synovium contains abundant PD-1^{hi}CD4$^+$ T cells that are distinct from T_{FH} cells.

Notably, PD-1^{hi}CXCR5$^-$CD4$^+$ T cells with a similar multidimensional phenotype, including increased expression of MHC II and ICOS, also appeared in the circulation, albeit at much lower frequencies (Extended Data Figs 1c, e, 2a, b). Quantification of circulating memory PD-1^{hi}CXCR5$^-$CD4$^+$ T cells in patients with established seropositive RA, seronegative RA, spondyloarthropathy, and non-inflammatory controls demonstrated a significantly increased frequency of PD-1^{hi}CXCR5$^-$ cells specifically in patients with seropositive RA (Fig. 1e, Extended Data Table 2). PD-1^{hi}CXCR5$^-$MHC-II$^+$ and PD-1^{hi}CXCR5$^-$ICOS$^+$ cells were also increased in blood of seropositive RA patients (Extended Data Fig. 2c). By contrast, the frequencies of

[1]Division of Rheumatology, Immunology, and Allergy, Brigham and Women's Hospital and Harvard Medical School, Boston, Massachusetts 02115, USA. [2]Rheumatology Research Group, Institute of Inflammation and Ageing, University of Birmingham, Queen Elizabeth Hospital, Birmingham B15 2WB, UK. [3]Division of Genetics, Brigham and Women's Hospital and Harvard Medical School, Boston, Massachusetts 02115, USA. [4]Program in Medical and Population Genetics, Broad Institute of Massachusetts Technical Institute and Harvard University, Cambridge, Massachusetts 02138, USA. [5]Partners Center for Personalized Genetic Medicine, Boston, Massachusetts 02115, USA. [6]Bioinformatics and Integrative Genomics, Harvard University, Cambridge, Massachusetts 02138, USA. [7]Biological and Biomedical Sciences, Harvard University, Cambridge, Massachusetts 02138, USA. [8]Arthritis and Tissue Degeneration Program, Hospital for Special Surgery, New York, New York 10021, USA. [9]David Z. Rosensweig Genomics Research Center, Hospital for Special Surgery, New York, New York 10021, USA. [10]Division of Immunology, Boston Children's Hospital, Boston, Massachusetts 02115, USA. [11]Division of Rheumatology, Hospital for Special Surgery, 535 E 70th Street, New York, New York 10021, USA. [12]Department of Medicine, Weill Cornell Medical College, Cornell University, New York, New York 10021, USA. [13]Autoimmunity and Inflammation Program, Hospital for Special Surgery, New York, New York 10021, USA. [14]Department of Surgery, Brigham and Women's Hospital, Boston, Massachusetts 02115, USA. [15]Reumatology Unit, Karolinska Institutet and Karolinska University Hospital Solna, Stockholm, S-171 76, Sweden. [16]Institute of Inflammation and Repair, University of Manchester, Manchester, M13 9PT, UK.

© 2017 Macmillan Publishers Limited, part of Springer Nature. All rights reserved.

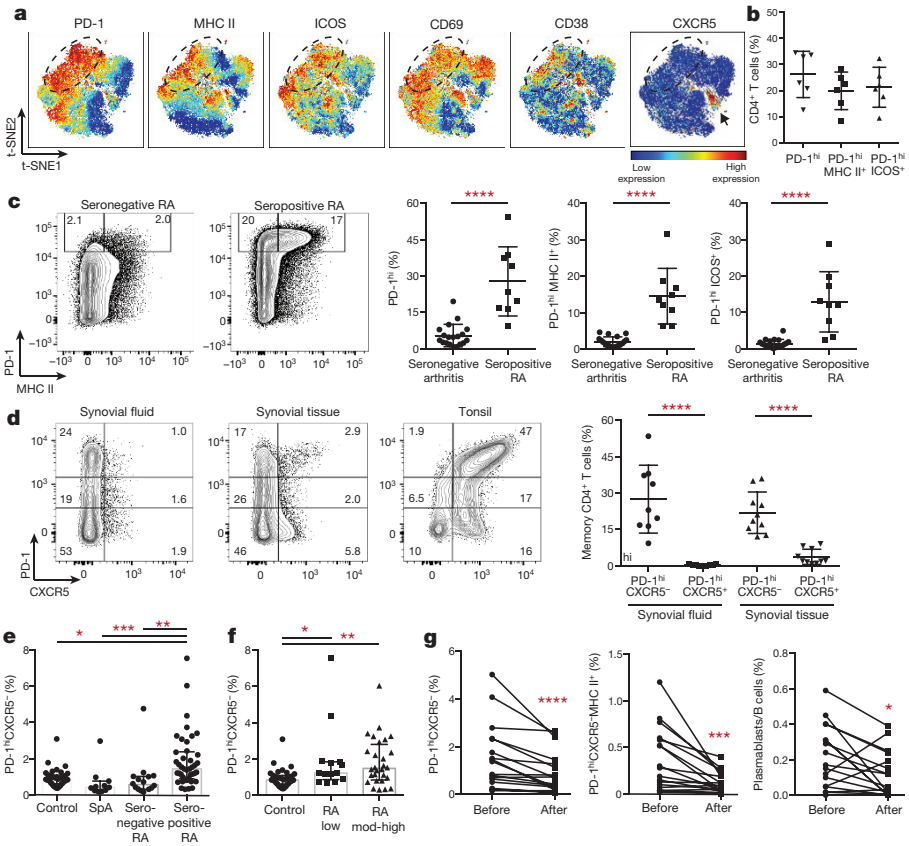

Figure 1 | Expanded PD-1^{hi}CXCR5^{-}CD4^{+} T cells in joints and blood of patients with seropositive RA. a, viSNE plots of mass cytometry of RA synovial tissue total CD4^{+} T cells. Colour indicates cell expression level of labelled marker. Circle demonstrates PD-1^{hi} cells. Arrow indicates CXCR5^{+} cells. **b**, PD-1^{hi} T-cell frequency in RA synovial tissue ($n = 6$). **c**, PD-1^{hi}CD4^{+} T-cell frequencies in synovial fluid from seropositive RA ($n = 9$) and seronegative inflammatory arthritides ($n = 19$). **d**, PD-1^{hi} cell frequencies in seropositive RA synovial fluid ($n = 9$) and tissue ($n = 10$). **e**, Percentage of PD-1^{hi}CXCR5^{-} cells within memory CD4^{+} T cells in seropositive RA ($n = 42$), seronegative RA ($n = 16$), spondyloarthropathy (SpA, $n = 11$), and control ($n = 35$) patient blood. **f**, PD-1^{hi} frequency in blood of seropositive RA patients with low ($n = 14$) or moderate–high ($n = 28$) disease activity. **g**, PD-1^{hi}CXCR5^{-}CD4^{+} T cell and plasmablast frequencies in blood before and after RA treatment escalation ($n = 18$). Mean ± s.d. (**b**–**d**), median ± interquartile range (**e**, **f**). $^{*}P < 0.05$, $^{**}P < 0.01$, $^{***}P < 0.001$, $^{****}P < 0.0001$ by Mann–Whitney (**c**, **d**), Kruskal–Wallis (**e**, **f**), Wilcoxon test (**g**).

PD-1^{hi}CXCR5^{+} cells and cells with intermediate PD-1 expression were not increased (Extended Data Fig. 2d, e).

PD-1^{hi}CXCR5^{-} cell frequencies were more robustly increased in seropositive RA patients with moderate or high disease activity (clinical disease activity index (CDAI) > 10) (Fig. 1f). The frequency of PD-1^{hi}CXCR5^{-} cells did not vary with other clinical parameters such as age, sex, disease duration, use of methotrexate or biologic therapies, or serum anti-CCP antibody titer (Extended Data Fig. 2f–h). In an independent cohort of 23 seropositive RA patients assayed before and after starting a new RA medication, there was a significant correlation between reduction in disease activity and reduction in the frequency of PD-1^{hi}CXCR5^{-} T cells (Extended Data Fig. 2i). The frequency of PD-1^{hi}CXCR5^{-} cells, PD-1^{hi}MHC-II^{+}CXCR5^{-} and PD-1^{hi}ICOS^{+}CXCR5^{-} cells decreased significantly in the 18 patients whose disease activity decreased after treatment escalation (Fig. 1g, Extended Data Fig. 2j).

As high PD-1 expression is often considered indicative of an exhausted state[8,9], we assessed the function of synovial PD-1^{hi}CXCR5^{-} cells. Surprisingly, despite a lack of CXCR5 expression, PD-1^{hi}CD4^{+} T cells sorted from seropositive RA synovial fluid showed a >100-fold increase in *IL21* mRNA expression and a >1,000-fold increase in *CXCL13* mRNA expression, as well as higher levels of *IFNG* and *IL10*, compared to PD-1^{-} T cells, with the highest expression in PD-1^{hi}MHC-II^{+} cells (Fig. 2a, sorted as in Extended Data Fig. 1e). By contrast, *IL2* showed a trend towards lower expression in PD-1^{hi} cells.

Consistent with mRNA expression, PD-1^{hi}CXCR5^{-} cells sorted from RA synovial fluid more frequently produced IL-21 (~30%), but less frequently produced IL-2, compared to PD-1^{-} or PD-1^{int} cells, after stimulation with PMA and ionomycin (Fig. 2b). Stimulation with anti-CD3/CD28 antibody beads induced greater CXCL13 production than did PMA and ionomycin. Notably, after anti-CD3/CD28 antibody stimulation, ~25% of PD-1^{hi}CXCR5^{-} cells produced CXCL13, but not IL-2, compared to <1% of PD-1^{-} or PD-1^{int} cells (Fig. 2b). High IL-21 and CXCL13 production by synovial fluid PD-1^{hi}CXCR5^{-}CD4^{+} T cells indicates that these cells are not globally exhausted, and instead suggests a possible B-cell helper function.

PD-1^{hi}MHC-II^{+} cells in seropositive RA synovial fluid also expressed high mRNA levels of the transcription factors MAF and BATF and the signalling adaptor SAP (encoded by *SH2D1A*), three factors important for T_{FH} cell development or function[3] (Extended Data Fig. 3a). However, BCL6, a transcription factor characteristically expressed in T_{FH} cells, was not elevated in synovial fluid PD-1^{hi} cells, whereas BLIMP1, a transcription factor typically downregulated in T_{FH} cells, was upregulated[3,10] (Extended Data Fig. 3a).

Intracellular flow cytometry confirmed that BLIMP1 was significantly elevated in PD-1^{hi}CXCR5^{-} cells, but not PD-1^{hi}CXCR5^{+} cells, from seropositive RA synovial samples (Fig. 2c, d). By contrast, BCL6 was markedly elevated in PD-1^{hi}CXCR5^{+} cells, such that the BCL6/BLIMP1 ratio was uniquely elevated in synovial PD-1^{hi}CXCR5^{+} cells. Expression of MAF, a factor that promotes IL-21 production

© 2017 Macmillan Publishers Limited, part of Springer Nature. All rights reserved.

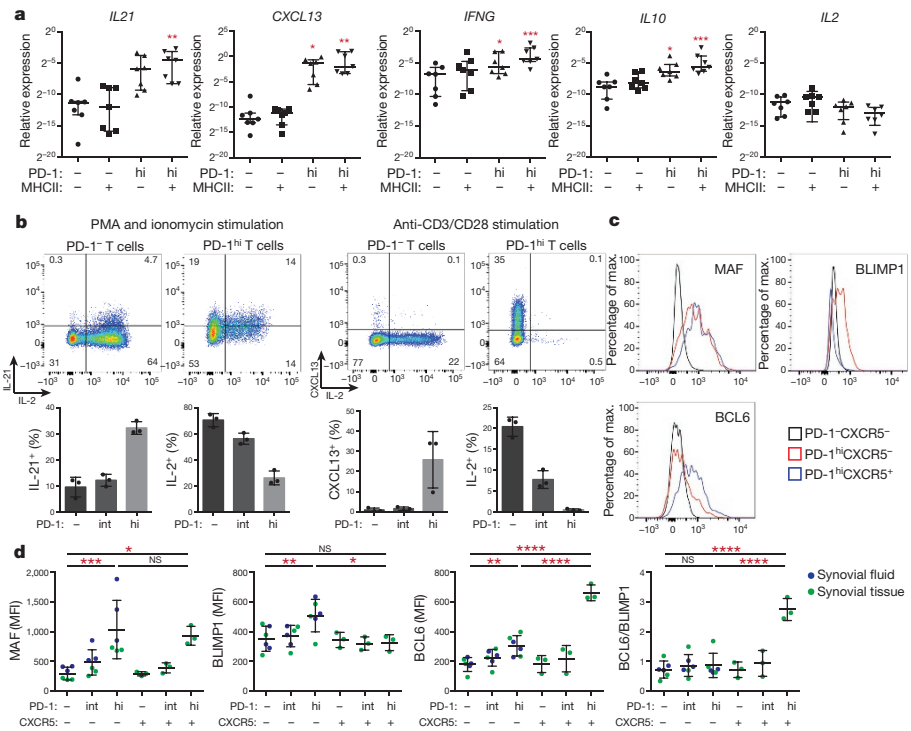

Figure 2 | Synovial PD-1^{hi}CXCR5^{-}CD4^{+} T cells express factors associated with B-cell help. a, Reverse transcription PCR of cytokines in memory CD4^{+} T-cell populations from RA synovial fluid ($n = 7$ donors). Median ± interquartile range. **b**, Cytokine production by synovial fluid memory CD4^{+} T cells ($n = 3$ experiments using different donors). **c**, Transcription factor expression in synovial tissue memory CD4^{+} T cells by flow cytometry. **d**, Quantification of transcription factor expression in T cells from synovial fluid (blue, $n = 3$ donors) or synovial tissue (green, $n = 3$ donors). Mean ± s.d. (**b**, **d**). $^{*}P < 0.05$, $^{**}P < 0.01$, $^{***}P < 0.001$, $^{****}P < 0.0001$ by Friedman's test compared to PD-1^{-}MHC-II^{-} cells (**a**) or one-way ANOVA comparing PD-1^{-}CXCR5^{-}, PD-1^{hi}CXCR5^{-}, and PD-1^{hi}CXCR5^{+} (**d**).

in human CD4^{+} T cells[11], was elevated in both PD-1^{hi}CXCR5^{-} and PD-1^{hi}CXCR5^{+} cells.

PD-1^{hi} memory CD4^{+} T cells from peripheral blood showed a transcriptional pattern similar to that in synovial fluid PD-1^{hi} cells, with increased expression of *IL21*, *CXCL13*, *IFNG*, *MAF*, *SAP*, and *BLIMP1*, but not *IL2* or *BCL6*, in circulating PD-1^{hi}MHC-II^{+} cells compared to PD-1^{-} cells (Extended Data Fig. 3b, c). Both PD-1^{hi}CXCR5^{-} and PD-1^{hi}CXCR5^{+} cells expressed increased IL-21 and CXCL13 and decreased IL-2 compared to PD-1^{-} T cells (Extended Data Fig. 3c). However, BLIMP1 expression was approximately threefold higher in PD-1^{hi}CXCR5^{-} compared to PD-1^{hi}CXCR5^{+} blood cells. Consistently, after *in vitro* stimulation, blood PD-1^{hi}CXCR5^{-} cells expressed more BLIMP1 and less BCL6 protein than did PD-1^{hi}CXCR5^{+} cells (Extended Data Fig. 3d). Taken together, these results indicate that both synovial and blood PD-1^{hi}CXCR5^{-} cells express factors associated with B-cell helper function without an elevated BCL6/BLIMP1 expression ratio.

To compare PD-1^{hi}CXCR5^{-} and PD-1^{hi}CXCR5^{+} cells more broadly, we analysed PD-1^{hi} cells from blood by mass cytometry (Extended Data Table 1). viSNE visualization of memory CD4^{+} T cells clustered PD-1^{hi}CXCR5^{-} and PD-1^{hi}CXCR5^{+} cells in close proximity, indicating a similar multidimensional phenotype (Fig. 3a, Extended Data Fig. 4a). By contrast, FoxP3^{+} regulatory T cells aggregated in a separate region, indicating that most PD-1^{hi} cells are not regulatory T cells, a finding confirmed by flow cytometry (Fig. 3a, Extended Data Fig. 4b).

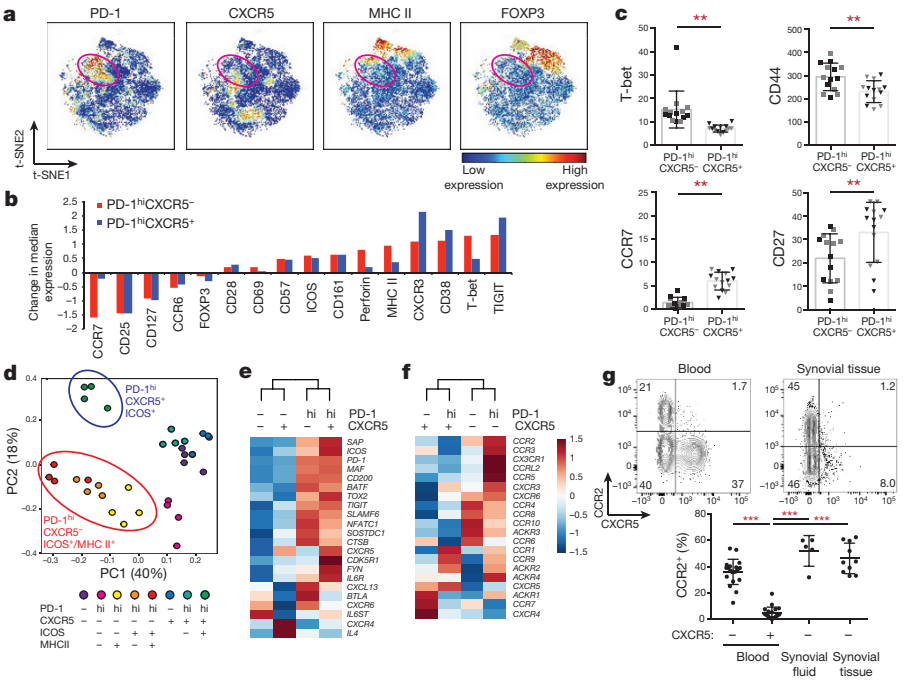

Figure 3 | High-dimensional analyses of PD-1^{hi}CXCR5^{-} and PD-1^{hi}CXCR5^{+} cells identify shared and distinct features. a, viSNE plots of blood memory CD4^{+} T cells from a patient with RA. Circle indicates PD-1^{hi} cells. **b**, Difference in expression of significantly altered proteins between PD-1^{hi} populations and PD-1^{-}CXCR5^{-} cells ($n = 14$ RA patients). **c**, Expression of indicated proteins by mass cytometry ($n = 7$ RA patients (black) and 7 controls (grey)). **d**, PCA of RNA-seq transcriptomes ($n = 4$ RA patients). **e**, **f**, Heat map of expression of T_{FH}-associated genes (**e**) or chemokine receptors (**f**). **g**, CCR2 expression on PD-1^{hi}CD4^{+} T cells by flow cytometry (blood $n = 20$, fluid $n = 5$, tissue $n = 10$). Mean ± s.d. shown. $^{**}P < 0.001$, $^{***}P < 0.0001$ by Wilcoxon (**c**), Kruskal–Wallis test (**g**).

© 2017 Macmillan Publishers Limited, part of Springer Nature. All rights reserved.

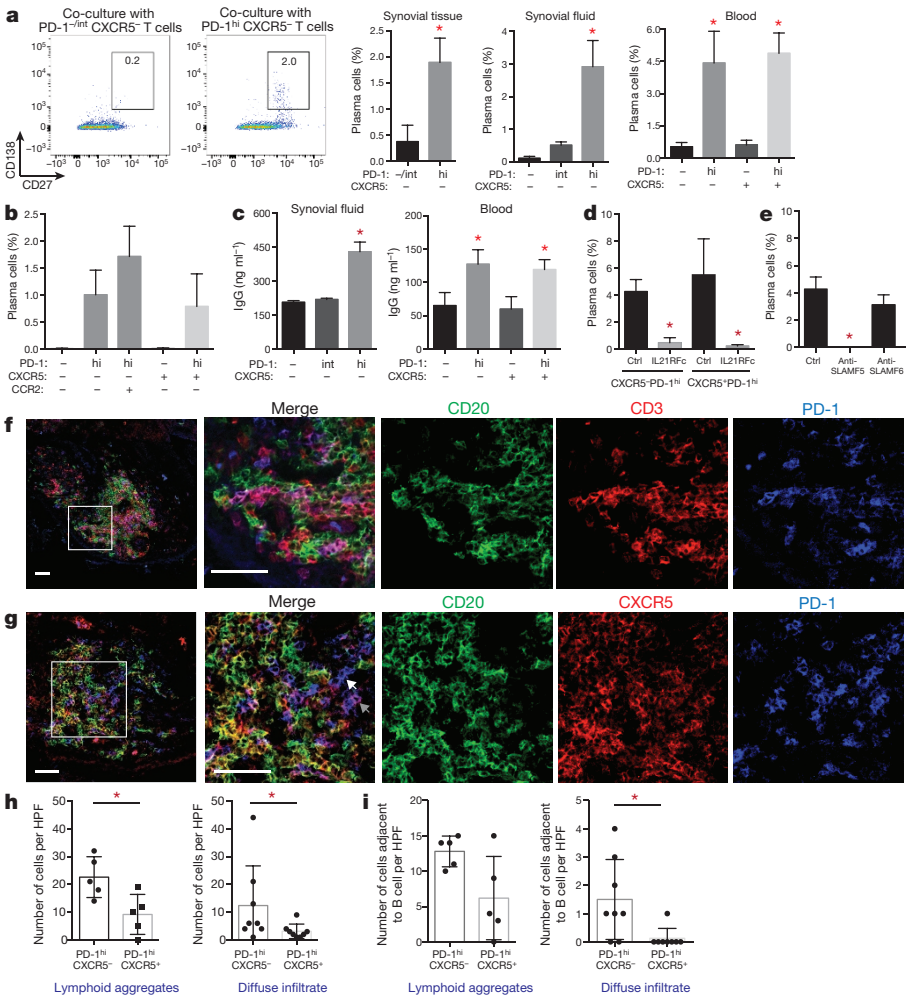

Figure 4 | PD-1^{hi}CXCR5^{-}CD4^{+} T cells promote plasma cell differentiation through IL-21 and SLAMF5 interactions. a, Plasma cell frequency in T–B-cell co-cultures using memory CD4^{+} T cells from indicated sources. Pooled data from 2 experiments (synovial tissue, $n = 3$ replicates per experiment), 3 experiments (synovial fluid), or 6 experiments (blood) using different donors. **b**, Co-cultures as in **a** using blood T-cell subpopulations. **c**, IgG in supernatants of co-cultures. **d**, **e**, Co-cultures with IL-21R–Ig fusion protein (**d**) or anti-SLAMF5/SLAMF6 antibody (**e**). For **b**–**e**, 1 of 3 experiments with different donors ($n = 3$ replicates). **f**, **g**, Immunofluorescence microscopy of RA synovium showing PD-1^{hi}CXCR5^{-} cells (white arrow) and a PD-1^{hi}CXCR5^{+} cell (grey arrow). Scale bar, 50 μm. **h**, **i**, Quantification of PD-1^{hi} cells in RA synovium ($n = 5$–8 high-power fields (HPF) from 4 samples). Mean ± s.d. shown. $^{*}P < 0.05$, $^{**}P < 0.01$, $^{***}P < 0.001$ by Mann–Whitney (**a** (synovial tissue), **d**), Kruskal–Wallis compared to PD-1^{-}CXCR5^{-} (**a** (blood, synovial fluid), **c**, **e**), or Wilcoxon test (**h**, **i**).

Both PD-1^{hi}CXCR5^{-} cells and PD-1^{hi}CXCR5^{+} cells showed significantly increased expression of 11 proteins, including TIGIT, ICOS, CD38, and CD57, and significantly decreased expression of 5 proteins, including CD25 and CD127, compared to PD-1^{-}CXCR5^{-} cells (Fig. 3b). Unlike TIGIT, the inhibitory receptors TIM-3, LAG-3, and CTLA-4 did not appear to be enriched on PD-1^{hi}CXCR5^{-} cells (Extended Data Fig. 4c). Compared to PD-1^{hi}CXCR5^{+} cells, PD-1^{hi}CXCR5^{-} cells showed lower expression of CCR7 and CD27 but higher CD44 and T-bet (Fig. 3b, c), suggesting a potentially distinct migratory capacity[12,13].

We next performed an unbiased global transcriptomic comparison of blood PD-1^{hi}CXCR5^{-} and PD-1^{hi}CXCR5^{+} cell subpopulations by RNA-seq. Principal components analysis separated PD-1^{hi} populations that co-expressed ICOS and/or MHC-II from PD-1^{-} cells along the first principal component (PC), irrespective of CXCR5 expression (Fig. 3d, Extended Data Fig. 4d). However, PD-1^{hi}CXCR5^{-} and PD-1^{hi}CXCR5^{+} cell populations were largely distinguished by PC2, indicating considerable differences in the global transcriptomes of PD-1^{hi}CXCR5^{-} cells and PD-1^{hi}CXCR5^{+} cells beyond CXCR5 expression alone.

Sixty-six genes were differentially expressed when comparing all of the PD-1^{hi} populations to the PD-1^{-} populations (log fold change >1.2, FDR <0.01, Extended Data Table 3), including a set of genes previously reported to be elevated in T_{FH} cells, such as *MAF*, *TIGIT*, and *SLAMF6* (refs 14, 15). Analysis of a curated list of T_{FH}-associated genes[14,16,17] demonstrated similar upregulation of multiple genes in the pooled PD-1^{hi}CXCR5^{+} cell samples and PD-1^{hi}CXCR5^{-} cell samples (Fig. 3e). When all eight subpopulations were analysed without pooling, hierarchical clustering based on these genes perfectly segregated PD-1^{hi} populations from PD-1^{-} populations, regardless of CXCR5 expression ($P < 0.026$, Extended Data Fig. 4e). These results highlight a shared transcriptional program associated with B-cell-helper function in PD-1^{hi}CXCR5^{-} cells and T_{FH} cells.

However, we also identified 16 genes with significantly different expression between PD-1^{hi}CXCR5^{-} and PD-1^{hi}CXCR5^{+} cells (Extended Data Table 4). Notably, PD-1^{hi}CXCR5^{-} cells showed 34-fold increased expression of *CCR2*, which encodes a chemokine receptor that mediates migration to sites of peripheral inflammation[18]. A targeted analysis of chemokine receptor expression on PD-1^{hi}CXCR5^{-} cells demonstrated marked upregulation of a set of 'inflammatory' chemokine receptors on these cells, including CCR2, CX3CR1, and CCR5, which was confirmed by flow cytometry[19] (Fig. 3f, g, Extended Data Fig. 4f). Notably, ~50% of PD-1^{hi}CXCR5^{-} cells in synovial tissue and synovial fluid from patients with seropositive RA expressed CCR2 (Fig. 3g). These results indicate that PD-1^{hi}CXCR5^{-} cells can be distinguished from PD-1^{hi}CXCR5^{+} cells not only by the lack of CXCR5 but also by high expression of inflammatory chemokine receptors.

To investigate the interconversion of PD-1^{hi} cells that express distinct chemokine receptors, PD-1^{hi}CXCR5^{-}CCR2^{-}, PD-1^{hi}CXCR5^{-}CCR2^{+}, and PD-1^{hi}CXCR5^{+}CCR2^{-} cell populations sorted from blood were stimulated *in vitro* and re-evaluated at different time points (Extended Data Fig. 5a, b). After 7 days, the majority of PD-1^{hi} cells that began as CXCR5^{-}CCR2^{+} cells remained CCR2^{+}, whereas less than 5% of these cells acquired CXCR5 (Extended Data Fig. 5c, d). Conversely, most PD-1^{hi} cells that began as CXCR5^{+}CCR2^{-} remained CXCR5^{+}, and less than 5% of these cells acquired CCR2. These results suggest that CXCR5 and CCR2 expression remain persistent, distinguishing features on PD-1^{hi}CD4^{+} T cells *in vitro*.

© 2017 Macmillan Publishers Limited, part of Springer Nature. All rights reserved.

We next tested directly whether PD-1^{hi}CXCR5^{-}CD4^{+} T cells can provide B-cell help *in vitro*. PD-1^{hi}CXCR5^{-} cells sorted from synovial tissue or synovial fluid from patients with seropositive RA induced differentiation of co-cultured memory B cells into plasma cells, whereas CXCR5^{-} cells without high PD-1 expression did not (Fig. 4a). The limited number of CXCR5^{+} T cells in synovial samples precluded comparison with PD-1^{hi}CXCR5^{+} cells. PD-1^{hi}CXCR5^{-} cells from blood also induced memory B-cell differentiation into plasma cells, with comparable activity in PD-1^{hi}CXCR5^{-}CCR2^{-}, PD-1^{hi}CXCR5^{-}CCR2^{+}, and PD-1^{hi}CXCR5^{+} cells (Fig. 4a, b). PD-1^{hi}CXCR5^{-} cells from synovial fluid and blood also enhanced IgG production in the co-cultures (Fig. 4c). Neutralization of IL-21 inhibited plasma cell differentiation induced by both blood PD-1^{hi}CXCR5^{-} cells and PD-1^{hi}CXCR5^{+} cells by ~90% (Fig. 4d). Expression of SLAMF5, a factor that is important for interactions between B cells and T cells[4], was elevated on both PD-1^{hi}CXCR5^{-} and PD-1^{hi}CXCR5^{+} cells, and antibody blockade of SLAMF5, but not SLAMF6, completely abrogated plasma cell differentiation and IgG production (Fig. 4e, Extended Data Fig. 6a–c). Consistent with a link *in vivo*, RA treatment escalation reduced the frequency of circulating plasmablasts in parallel with the reduction in PD-1^{hi}CXCR5^{-} T cells (Fig. 1g).

Finally, immunofluorescence microscopy identified CD3^{+} T cells with bright PD-1 expression in all four seropositive RA synovial samples analysed (Fig. 4f). CXCR5 was observed on CD20^{+} B cells and on a minority of PD-1^{hi} T cells that were enriched within lymphoid aggregates (Fig. 4g, h). However, PD-1^{hi}CXCR5^{-} cells outnumbered PD-1^{hi}CXCR5^{+} cells within lymphoid aggregates, and were around fourfold more abundant than PD-1^{hi}CXCR5^{+} cells in regions outside of lymphoid aggregates (Fig. 4h). Within lymphoid aggregates, both PD-1^{hi}CXCR5^{-} cells and PD-1^{hi}CXCR5^{+} cells were found adjacent to B cells (Fig. 4g, i). However, in areas outside of lymphoid aggregates, the majority of PD-1^{hi} cells adjacent to B cells were CXCR5^{-} (Fig. 4i, Extended Data Fig. 6d). These results suggest a unique capacity of PD-1^{hi}CXCR5^{-} T cells to interact with B cells both within lymphoid aggregates and more diffusely throughout the inflamed synovium.

Here, we have defined a PD-1^{hi}CXCR5^{-}CD4^{+} T 'peripheral helper' (T_{PH}) cell population markedly expanded in rheumatoid arthritis that combines B-cell-helper function with a migratory program targeting inflamed tissues. The abundance of T_{PH} cells in RA synovium highlights the importance of tissue-localized T–B-cell interactions[20]. T_{PH} cells may infiltrate chronically inflamed tissues, which would not be expected to readily recruit T_{FH} cells, providing a potential mechanism for the initiation of ectopic lymphoid structures[21–23]. T_{PH}-cell production of CXCL13 and IL-21 may recruit both T_{FH} and B cells, promoting local autoantibody production that may not be reflected in serum, and perhaps modulating other B-cell functions such as cytokine production[7,24]. Identification of the T_{PH} cell phenotype considerably expands the spectrum of B-cell-helper T cells that may be assessed as biomarkers for autoantibody-associated diseases. Further, high expression of PD-1 on T_{PH} cells may offer a potential strategy for therapeutic targeting of tissue T–B-cell interactions.

Online Content Methods, along with any additional Extended Data display items and Source Data, are available in the online version of the paper; references unique to these sections appear only in the online paper.

Received 19 April; accepted 18 November 2016.

1. Maecker, H. T., McCoy, J. P. & Nussenblatt, R. Standardizing immunophenotyping for the Human Immunology Project. *Nat. Rev. Immunol.* **12,** 191–200 (2012).
2. McInnes, I. B. & Schett, G. The pathogenesis of rheumatoid arthritis. *NEJM* **365,** 2205–2219 (2011).
3. Crotty, S. Follicular helper CD4 T cells (T_{FH}). *Annu. Rev. Immunol.* **29,** 621–663 (2011).
4. Cannons, J. L. *et al.* Optimal germinal center responses require a multistage T cell:B cell adhesion process involving integrins, SLAM-associated protein, and CD84. *Immunity* **32,** 253–265 (2010).
5. Amir, A. D. *et al.* viSNE enables visualization of high dimensional single-cell data and reveals phenotypic heterogeneity of leukemia. *Nat. Biotechnol.* **31,** 545–552 (2013).
6. Takemura, S. *et al.* Lymphoid neogenesis in rheumatoid synovitis. *J. Immunol.* **167,** 1072–1080 (2001).
7. Humby, F. *et al.* Ectopic lymphoid structures support ongoing production of class-switched autoantibodies in rheumatoid synovium. *PLoS Med.* **6,** e1 (2009).
8. Wherry, E. J. & Kurachi, M. Molecular and cellular insights into T cell exhaustion. *Nat. Rev. Immunol.* **15,** 486–499 (2015).
9. Kamphorst, A. O. & Ahmed, R. Manipulating the PD-1 pathway to improve immunity. *Curr. Opin. Immunol.* **25,** 381–388 (2013).
10. Johnston, R. J. *et al.* Bcl6 and Blimp-1 are reciprocal and antagonistic regulators of T follicular helper cell differentiation. *Science* **325,** 1006–1010 (2009).
11. Kroenke, M. A. *et al.* Bcl6 and Maf cooperate to instruct human follicular helper CD4 T cell differentiation. *J. Immunol.* **188,** 3734–3744 (2012).
12. DeGrendele, H. C., Estess, P. & Siegelman, M. H. Requirement for CD44 in activated T cell extravasation into an inflammatory site. *Science* **278,** 672–675 (1997).
13. Förster, R. *et al.* CCR7 coordinates the primary immune response by establishing functional microenvironments in secondary lymphoid organs. *Cell* **99,** 23–33 (1999).
14. Chtanova, T. *et al.* T follicular helper cells express a distinctive transcriptional profile, reflecting their role as non-T_H1/T_H2 effector cells that provide help for B cells. *J. Immunol.* **173,** 68–78 (2004).
15. Locci, M. *et al.* Human circulating PD-1^{+}CXCR3^{-}CXCR5^{+} memory T_{FH} cells are highly functional and correlate with broadly neutralizing HIV antibody responses. *Immunity* **39,** 758–769 (2013).
16. Weinstein, J. S. *et al.* Global transcriptome analysis and enhancer landscape of human primary T follicular helper and T effector lymphocytes. *Blood* **124,** 3719–3729 (2014).
17. Kenefeck, R. *et al.* Follicular helper T cell signature in type 1 diabetes. *J. Clin. Invest.* **125,** 292–303 (2015).
18. Kuziel, W. A. *et al.* Severe reduction in leukocyte adhesion and monocyte extravasation in mice deficient in CC chemokine receptor 2. *Proc. Natl Acad. Sci. USA* **94,** 12053–12058 (1997).
19. Rot, A. & von Andrian, U. H. Chemokines in innate and adaptive host defense: basic chemokinese grammar for immune cells. *Annu. Rev. Immunol.* **22,** 891–928 (2004).
20. Vu Van, D. *et al.* Local T/B cooperation in inflamed tissues is supported by T follicular helper-like cells. *Nat. Commun.* **7,** 10875 (2016).
21. Pitzalis, C., Jones, G. W., Bombardieri, M. & Jones, S. A. Ectopic lymphoid-like structures in infection, cancer and autoimmunity. *Nat. Rev. Immunol.* **14,** 447–462 (2014).
22. Kobayashi, S. *et al.* A distinct human CD4^{+} T cell subset that secretes CXCL13 in rheumatoid synovium. *Arthritis Rheum.* **65,** 3063–3072 (2013).
23. Manzo, A. *et al.* Mature antigen-experienced T helper cells synthesize and secrete the B cell chemoattractant CXCL13 in the inflammatory environment of the rheumatoid joint. *Arthritis Rheum.* **58,** 3377–3387 (2008).
24. Shen, P. & Fillatreau, S. Antibody-independent functions of B cells: a focus on cytokines. *Nat. Rev. Immunol.* **15,** 441–451 (2015).

Acknowledgements This work was supported by T32 AR007530-31 and the William Docken Inflammatory Autoimmune Disease Fund (to M.B.B.), Mallinckrodt Research Fellowship (to D.A.R.), R01 AR064850-03 (to Y.C.L.), NIH 5U01GM092691-05, 1U19 AI111224-01 and Doris Duke Charitable Foundation Grant #2013097 (to S.R.), Rheumatology Research Foundation Scientist Development Award (to L.A.H.), K01 AR066063 (to L.T.D.), Arthritis Research UK programme grant #19791 (to C.D.B.), and Arthritis Research UK Clinician Scientist Fellowship #18547 (to A.F.). J.L.M was supported by the FP7-HEALTH-F2-2012-305549 EuroTEAM. P.A.N. was supported by P30 AR070253 and the Fundación Bechara. We thank A. Chicoine and the BWH Human Immunology Center Flow Cytometry Core for assistance with cell sorting.

Author Contributions D.A.R conceived the project, performed experiments, analysed data, and wrote the manuscript. M.F.G., Y.L., N.T., and F.M. performed experiments and analysed data. K.S. analysed transcriptomic data. C.F. analysed mass cytometry data. J.L.M. performed immunofluorescence microscopy. J.A.L. assisted with mass cytometry. K.W., L.A.H., P.A.N., M.E.W., Y.C.L., J.S.C., D.J.T., E.M.M., S.M.H., E.W.K., L.T.D., V.P.B., L.B.I., S.M.G., A.B.P., A.F. and C.D.B participated in study design, patient recruitment and sample acquisition. M.B.B. and S.R. conceived the project, supervised the work, analysed data, and co-wrote the manuscript. All authors discussed the results and commented on the manuscript.

Author Information Reprints and permissions information is available at www.nature.com/reprints. The authors declare no competing financial interests. Readers are welcome to comment on the online version of the paper. Correspondence and requests for materials should be addressed to M.B.B. (mbrenner@research.bwh.harvard.edu) or D.A.R. (darao@partners.org).

Reviewer Information *Nature* thanks J. Craft, S. Fillatreau and the other anonymous reviewer(s) for their contribution to the peer review of this work.

© 2017 Macmillan Publishers Limited, part of Springer Nature. All rights reserved.

METHODS

Data reporting. No statistical methods were used to predetermine sample size. The experiments were not randomized and the investigators were not blinded to allocation during experiments and outcome assessment.

Human research. Research involving human subjects was performed according to the Institutional Review Boards at Partners HealthCare, Hospital for Special Surgery, or the University of Birmingham Local Ethical Review Committee (Birmingham, UK) through approved protocols with appropriate informed consent as required. Patients with RA fulfilled the ACR 2010 Rheumatoid Arthritis classification criteria. Rheumatoid factor and anti-CCP antibody status, C-reactive protein level, and medication usage were obtained by review of electronic medical records. Biologic therapy was defined as use of anti-TNF, abatacept, rituximab, tocilizumab, or tofacitinib. Synovial tissue samples for mass and flow cytometry were collected from patients with seropositive RA that were undergoing arthroplasty at the Hospital for Special Surgery, New York or at Brigham and Women's Hospital, Boston. Samples with lymphocytic infiltrates on histology were prioritized for analyses. Synovial tissue for microscopy was acquired by synovial biopsy of a clinically inflamed joint from seropositive RA patients within the Birmingham early arthritis cohort (BEACON) at the University of Birmingham, UK.

Synovial fluid samples were obtained as excess material from a separate cohort of patients undergoing diagnostic or therapeutic arthrocentesis of an inflammatory knee effusion as directed by the treating rheumatologist. These samples were de-identified; therefore, additional clinical information was not available, except for the three patients from whom paired synovial fluid and blood were obtained.

Blood samples for clinical phenotyping were obtained from patients seen at the Brigham and Women's Hospital Arthritis Center. For blood cell analyses in the cross-sectional cohort, CDAI was measured by the treating clinician on the day of sample acquisition. Anti-CCP titers were measured using the Immunoscan CCPLus ELISA (Eurodiagnostica), with a positive result defined as >25 units per ml. For patients with RA that were followed longitudinally, a new treatment was initiated at the discretion of the treating physician, and CDAIs were determined at each visit by trained research study staff. Blood samples were acquired before initiation of a new biologic therapy or within 1 week of starting methotrexate. Concurrent prednisone at doses $\leq 10\,mg\,d^{-1}$ were permitted.

All synovial fluid and blood samples were subjected to density centrifugation using Ficoll-Hypaque to isolate mononuclear cells, which were cryopreserved for batched analyses. Most phenotypic and transcriptomic analyses of blood T cells were performed on samples from both RA patients and non-inflammatory controls, with similar results unless specifically indicated. *In vitro* PD-1^{hi} T cell interconversion assays and *in vitro* B-cell-helper assays using T cells from the blood were performed using PBMC from blood bank leukoreduction collars from anonymous donors.

All blood $CD4^+$ T cell analyses included only $CD45RA^-$ memory $CD4^+$ T cells, except where naive ($CD45RA^+$) cells are specifically indicated. Here the term 'memory' is used to denote an 'antigen-experienced' status indicated by loss of the naive T-cell marker CD45RA. This population includes both resting and activated antigen-experienced T cells. Synovial fluid and tissue analyses also utilize only memory $CD4^+$ T cells unless total $CD4^+$ T cells are indicated. Naive T cells constituted <10% of the total population of $CD4^+$ T cells in synovial tissue and synovial fluid.

Synovial tissue analysis. Synovial samples were acquired from discarded arthroplasty tissue. Synovial tissue was isolated by careful dissection, minced, and digested with $100\,\mu g\,ml^{-1}$ LiberaseTL and $100\,\mu g\,ml^{-1}$ DNaseI (both Roche) in RPMI (Life Technologies) for 15 min, inverting every 5 min. Cells were passed through a 70-μm cell strainer, washed, subjected to red blood cell lysis, and cryopreserved in Cryostor CS10 (BioLife Solutions) for batched analyses.

Mass cytometry. Cryopreserved disaggregated synovial cells or PBMCs were thawed into RPMI and 10% FBS (HyClone). Viability was assessed with rhodium for PBMCs and cisplatin (both Fluidigm) for synovial cells. Cells were then washed and stained with primary antibody cocktails at 1:100 dilution (Extended Data Table 1). All antibodies were obtained from the Longwood Medical Area CyTOF Antibody Resource Core (Boston, Massachusetts). Cells were then washed, fixed and permeabilized using the Ebioscience Transcription Factor Fix/Perm Buffer for 45 min, washed in PBS/1% BSA/0.3% saponin, then stained for intracellular markers. Cells were re-fixed in formalin (Sigma), washed with Milli-Q water, and analysed on a CyTOF2 (Fluidigm) for PBMC or Helios (Fluidigm) for synovial cells. Mass cytometry data were normalized using EQ Four Element Calibration Beads (Fluidigm) as described[25].

viSNE analyses were performed on cytometry data from 3 of 6 synovial tissue samples, 3 of 9 synovial fluid samples, and 8 of 14 blood samples using the Barnes–Hut SNE implementation on Cytobank (http://www.cytobank.org). All three individual synovial tissue sample analyses are shown. For synovial fluid and blood cell analyses, one representative patient sample is shown. For synovial tissue mass cytometry data, gated $CD4^+$ T cells were analysed using all available protein markers, and each synovial tissue sample was analysed individually to allow for maximal resolution. For paired synovial fluid and blood flow cytometry data, gated memory $CD4^+$ T cells from synovial fluid and blood were analysed together in a single viSNE analysis for direct comparison using an equal number of randomly selected cells from each sample. For blood mass cytometry analyses, equal numbers of gated memory $CD4^+$ T cells from each sample were analysed together using all markers except those used for gating (CD3, CD4, CD45RO). Comparison of marker expression on PD-$1^{hi}CXCR5^-$ and PD-$1^{hi}CXCR5^+$ cells was performed with R-3.2 using Mann–Whitney tests and *P* values were adjusted for multiple testing using the Bonferroni correction. Mass cytometry data were transformed using the inverse hyperbolic sine before expression analysis[25] as in Fig. 3b.

Flow cytometry and cell sorting. For PD-1^{hi} T-cell quantification, cryopreserved cells were thawed into warm RPMI/10% FBS, washed once in cold PBS, and stained in PBS/1% BSA with the following antibodies for 45 min: anti-CD27-FITC (TB01), anti-CXCR3-PE (CEW33D), anti-CD4-PE-Cy7 (RPA-T4), anti-ICOS-PerCP-Cy5.5 (ISA-3), anti-CXCR5-BV421 (J252D4), anti-CD45RA-BV510 (HI100), anti-HLA-DR-BV605 (G46-6), anti-CD49d-BV711 (9F10), anti-PD-1-APC (EH12.2H7), anti-CD3-AlexaFluor700 (HIT3A), anti-CD29-APC-Cy7 (TS2/16), propidium iodide. Antibodies used in additional panels included anti-SLAM-AF488 (A12), anti-SLAMF5-PE (CD84.1.21), anti-SLAMF6-PE (NT-7), anti-CCR2-PE (K036C2), anti-CX3CR1-FITC (2A9-1), anti-CD38-PE (HIT2), anti-CD138-PE/Cy7 (MI15), anti-CTLA-4-PerCP/Cy5.5 (L3D10) from BioLegend, anti-CCR5-FITC (2D7) and anti-FoxP3-AF647 (236A/E7) from BD Biosciences, anti-LAG-3-APC from R&D Systems, anti-TIM-3-PE/Cy7 (F38-2E2) and anti-TIGIT-PE (MBSA43) from eBioscience.

Cells were washed in cold PBS, passed through a 70-μm filter, and data acquired on a BD FACSAria Fusion, BD Fortessa, or BD Canto II analyser using FACSDiva software. Data were analysed using FlowJo 10.0.7. For blood cell quantification in Fig. 1 and Extended Data Fig. 2, samples were analysed in uniformly processed batches of coded samples with multiple disease conditions included in each batch. Upon data acquisition, disease categories were assigned to data files. A single set of gates for PD-1, CXCR5, ICOS, and MHC II was applied to all samples. The percentage of PD-1^{hi} T-cell populations among memory $CD4^+$ T-cells populations and the percentage of plasmablasts ($CD19^+CD20^{lo}CD38^{hi}CD27^+$) among total $CD19^+$ B cells were calculated for indicated samples.

T cells were sorted directly from synovial fluid and synovial tissue samples. For sorting blood T cells, total $CD4^+$ T cells were first isolated by magnetic bead negative selection (Miltenyi Biotec). Cell sorting was performed on a BD FACSAria Fusion sorter using a 70-μm nozzle. Sort gates were drawn as depicted in Extended Data Fig. 1e. Cell purity was routinely >98%. For functional analyses, cells were sorted into cold RPMI/10% FBS. For RNA analyses, sorted cells were lysed in RLT lysis buffer (Qiagen) with 1% β-mercaptoethanol (Sigma).

Intracellular cytokine staining. Synovial fluid mononuclear cells were stained with anti-PD-1-PE/Dazzle 594, CXCR5-BV605, and CD4-BV650 (Biolegend), and propidium iodide. $CXCR5^-$PD-1^{hi}, PD-1^{int}, and PD-1^-CD4^+ T cells sorted as above were pelleted by centrifugation and resuspended in RPMI/10% FBS at a density of 5×10^5 cells per ml in 24-well plates. Cells were stimulated with either anti-CD3/anti-CD28 beads at a ratio of 2:1 (cell:bead) for 24 h, or with phorbol 12-myristate 13-acetate (PMA, $50\,ng\,ml^{-1}$) and ionomycin ($1\,\mu g\,ml^{-1}$) for 6 h. Brefeldin A and monensin (both 1:1,000, eBioscience) were added for the last 5 h. Cells were washed twice in cold PBS, incubated for 30 min with Fixable Viability Dye eFluor 455UV (eBioscience), washed in PBS/1% BSA, and then fixed and permeabilized using the eBioscience Transcription Factor Fix/Perm Buffer. Cells were washed in PBS/1% BSA/0.3% saponin and incubated with anti-IL-21-APC (3A3-N2), anti-IL-2-PE/Cy7 (MQ1-17H12), and anti-CXCL13-AlexaFluor700 (53610, R&D Systems) for 30 min, washed once, filtered, and data acquired on a BD Fortessa analyser.

Intracellular transcription factor staining. Synovial tissue and synovial fluid cells were thawed, washed twice in PBS, and incubated with Fixable Viability Dye eFluor 455UV (eBioscience) for 30 min. Cells were then washed in PBS/1% BSA and stained with antibodies against surface markers anti-CD3-AF700, anti-CD4-BV650, anti-CCR2-PE, anti-CXCR5-BV421, anti-PD-1-PE/Dazzle 594 (all Biolegend) for 30 min. Cells were washed once and incubated with eBioscience Transcription Factor Fix/Perm Buffer. Cells were washed in PBS/1% BSA/0.3% saponin and incubated in intracellular antibodies anti-MAF-PerCP-eFluor710 (sym0F1, eBioscience), anti-Bcl6-APC (BCL-UP, eBioscience), and anti-Blimp-1-AF488 (646702, R&D Systems) at 1:20 dilutions for 4 h. Cells were washed once, filtered, and data acquired on a BD Fortessa analyser. Intracellular detection of FoxP3 and CTLA-4 were performed by the same

© 2017 Macmillan Publishers Limited, part of Springer Nature. All rights reserved.

method on magnetic-bead purified blood $CD4^+$ T cells using the indicated surface markers.

RT–PCR analyses. RNA was isolated using RNeasy Micro Kits (Qiagen). cDNA was prepared using Quantitect RT–PCR (Qiagen) and PCR performed with Brilliant III SYBRGreen on an a Stratagene Mx3000. Primers used were as follows: *RPL13A* (forward: 5′-CATAGGAAGCTGGGAGCAAG-3′; reverse: 5′-GCCCTCCAATCAGTCTTCTG-3′), *IL2* (forward: 5′-AGAACTCAAACCTCTGGAGGAAG-3′; reverse: 5′-GCTGTCTCAGCATATTCACAC-3′), *IFNG* (forward: 5′-GCATCGTTTTGGGTTCTCTTG-3′; reverse: 5′-AGTTCCATTATCCGCTACATCTG-3′), *IL10* (forward: 5′-CGCATGTGAACTCCCTGG-3′; reverse: 5′-TAGATGCCTTTCTCTTGGAGC-3′), *IL21* (forward: 5′-AGGAAACCACCTTCCACAAA-3′; reverse: 5′-GAATCACATGAAGGGCATGTT-3′), *CXCL13* (forward: 5′-TCTCTGCTTCTCATGCTGCT-3′; reverse: 5′-TCAAGCTTGTGTAATAGACCTCCA-3′), *PD1* (forward: 5′-CCAGGATGGTTCTTAGACTCC-3′; reverse: 5′-TTTAGCACGAAGCTCTCCGAT-3′), *CXCR5* (forward: 5′-GGGAGCCTCTCAACATAAGAC-3′; reverse: 5′-CCAATCTGTCCAGTTCCCAGA-3′), *MAF* (forward: 5′-CCGTCCTCTCCCGAGTTTTT-3′; reverse: 5′-TGCTGGGGCTTCCAAAATGT-3′), *BCL6* (forward: 5′-GTTTCCGGCACCTTCAGACT-3′; reverse: 5′-CTGGCTTTTGTGACGGAAAT-3′), *BATF* (forward: 5′-TGGCAAACAGGACTCATCTG-3′; reverse: 5′-CTGTTTCTCCAGGTCTTCGC-3′), *SAP* (forward: 5′-GCTATTTGCTGAGGGACAGC-3′; reverse: 5′-TGTCTGGGACACTCGGTATG-3′), *BLIMP1* (forward: 5′-AACTTCTTGTGTGGTATTGTCGG-3′; reverse: 5′-TCTCAGTGCTCGGTTGCTTT-3′). Expression levels relative to control gene *RPL13A* were calculated.

RNA sequencing. RNA was isolated from 800–1,000 cells from sorted T-cell subpopulations as described. 5 μl of total RNA were placed in wells of a 96-well plate and RNA sequencing libraries were prepared at Broad Technology Labs at the Broad Institute of Harvard and MIT using the Illumina SmartSeq2 platform. Samples were sequenced on a NextSeq500 using 75 bp paired-end reads to an average depth of 9 M pairs of reads per sample. All cDNA transcripts from Ensembl release 82 were quantified with Kallisto version 0.42.4 (ref. 26). We used limma to model each gene as a linear combination of donor-specific effects. The residuals from these models were tested by ANOVA across 8 gates, and 581 genes with a significant F statistic with <5% FDR were selected for PCA. Heat maps show row-normalized relative gene expression z-scores across columns (mean 0 and variance 1), with subpopulations of PD-1^{hi}CXCR5^- or PD-1^{hi}CXCR5^+ averaged to yield overall PD-1^{hi}CXCR5^- and PD-1^{hi}CXCR5^+ expression values. In comparisons of specific cell populations, genes with log fold change >1.2 and FDR <1% were considered differentially expressed.

PD-1^{hi} cell *in vitro* stimulation assays. $CD4^+$ T cells were purified from PBMCs from blood bank leukoreduction collars by magnetic bead negative selection and stained with anti-CD4-BV650, anti-CD45RA-BV510, anti-PD-1-APC, anti-CXCR5-BV605, and anti-CCR2-PE/Cy7. Naive $CD4^+$ T cells and memory $CD4^+$ T-cell subpopulations were sorted into RPMI/10% FBS. 50,000 cells were resuspended in RPMI/10% FBS at 0.25×10^6 cells ml^{-1} and cultured with anti-CD3/CD28 beads (Dynabeads) at a cell:bead ratio of 5:1 for 2 or 7 days. Cells were then either re-stained with anti-PD-1-PE and anti-CXCR5-BV421 antibodies and sorted into lysis buffer for RT–PCR analyses, or stained with anti-CCR2-PE and anti-CXCR5-BV421 and analysed by intracellular flow cytometry for transcription factors as above.

T–B-cell co-cultures. Total B cells were isolated first from PBMCs from blood bank leukoreduction collars by magnetic bead positive selection using CD19 (Miltenyi), then $CD4^+$ T cells were isolated by negative selection. B cells were stained with anti-CD14-APC, anti-CD3-PeCy7, and anti-CD27-BV510 antibodies (all from Biolegend), and memory B cells sorted as $CD27^+CD14^-CD3^-$ cells on a BD FACSAria Fusion to remove contaminating T cells and monocytes. Sorted T-cell populations were co-cultured with autologous memory B cells at a ratio of 1:10 in 100 μl of RPMI/10% FBS and stimulated with LPS (5 μg ml^{-1}) and SEB (1 μg ml^{-1}) for 7 days. For co-cultures using synovial tissue or synovial fluid T cells, allogeneic memory B cells from PBMC were used. Supernatants were collected and total IgG measured by ELISA (eBioscience). Cells were harvested and analysed by flow cytometry, with plasmablasts defined as $CD19^+CD20^{lo}CD38^{hi}CD27^+$ and plasma cells defined as $CD19^+CD20^{lo}CD38^{hi}CD27^+CD138^+$. For blocking experiments, 10 μg ml^{-1} anti-SLAMF5 or anti-SLAMF6 antibodies (Biolegend) or 20 μg ml^{-1} IL-21R–Ig (R&D Systems) were used.

Immunofluorescence microscopy. 6-μm sections of synovium frozen in OCT were fixed in acetone, rehydrated in PBS, and blocked with 10% normal goat serum before application of primary antibodies as follows: PD-1 (EH12.2H7, BioLegend), CD3 (SP7, Abcam), CD20 (L26, Dako), CXCR5 (MAB190, R&D Systems), all at a dilution of 1:100 except for CD20, which was used at 1:300. All secondary antibodies were raised in goat. CXCR5 was detected using anti mouse IgG2b biotin (Southern biotech) followed by streptavidin conjugated AlexaFluor 546 (Life Technologies), CD20 with anti-mouse IgG2a FITC (both Southern Biotech), PD-1 with anti-mouse IgG1 conjugated to AlexaFluor 647 and CD3 with anti-rabbit AlexaFluor 546 (both Life Technologies). FITC staining was amplified with anti-FITC AlexaFluor 488 (Life Technologies). Slides were mounted using ProLong Diamond (Life Technologies), left to cure overnight and imaged using a Zeiss LSM 780 confocal microscope. Images were processed using Zen Black (Zeiss) and then ImageJ. Cell counts were performed on images obtained from confocal imaging using the Cell Counter plugin for ImageJ (imagej.net/Cell_Counter). Synovial regions were categorized as 'lymphoid aggregates' when the B cells and T cells formed distinct clusters, and 'diffusely infiltrated' when B cells were loosely distributed within the synovium.

Statistical analyses. Statistical comparisons were performed as indicated in figure legends using two-sided tests. P values <0.05 were considered significant after adjusting for multiple testing using the Bonferroni correction for ANOVA (Fig. 2d) and blood mass cytometry analysis (Fig. 3b), or Dunn's test for non-parametric multi-group comparisons.

Data availability. The RNA-seq dataset is available at the ImmPort repository, accession number SDY939 (https://www.immport.org/immport-open/public/study/study/displayStudyDetail/SDY939). The data that support the findings of this study are available from the corresponding author upon reasonable request.

25. Finck, R. *et al.* Normalization of mass cytometry data with bead standards. *Cytometry A* **83,** 483–494 (2013).
26. Bray, N., Pimentel, H., Melsted, P. & Pachter, L. Near-optimal RNA-Seq quantification. Preprint at https://arxiv.org/abs/1505.02710 (2015).

© 2017 Macmillan Publishers Limited, part of Springer Nature. All rights reserved.

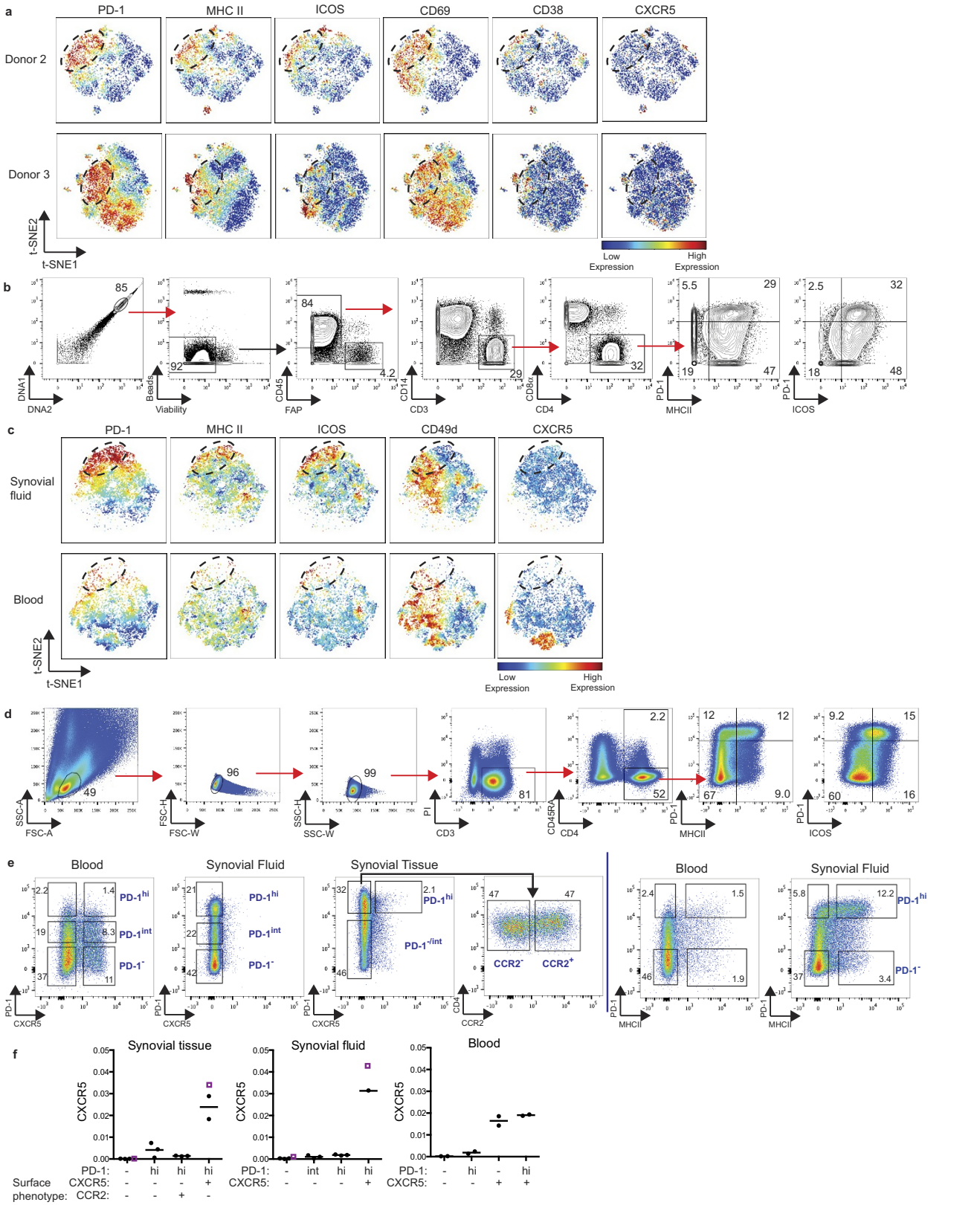

Extended Data Figure 1 | Detection of PD-1^{hi}CD4^{+} T cells in RA synovial tissue and fluid by mass and flow cytometry. a, viSNE plots of mass cytometry of RA synovial tissue CD4^{+} T cells as in Fig. 1a from 2 additional donors. **b**, Gating strategy to identify synovial tissue PD-1^{hi} CD4^{+} T cell populations by mass cytometry. **c**, viSNE plots of flow cytometry of paired RA synovial fluid and blood memory CD4^{+} T cells. **d**, Gating strategy to identify synovial fluid PD-1^{hi} memory CD4^{+} T cells by flow cytometry. **e**, Examples of gating used to sort memory CD4^{+} T cell populations from patient samples. **f**, Detection of CXCR5 mRNA by RT–PCR in sorted memory CD4^{+} T-cell populations from synovial tissue ($n = 3$ donors, 2 of which provided sufficient PD-1^{hi} CXCR5^{+} cells for analysis), synovial fluid ($n = 3$ donors, 1 of which provided sufficient PD-1^{hi} CXCR5^{+} cells for analysis), and blood ($n = 2$ donors). Purple boxes indicate PD-1^{-} and PD-1^{hi} CXCR5^{+} cells sorted from human tonsil as controls. Lines in **f** indicate mean for synovial or blood samples.

© 2017 Macmillan Publishers Limited, part of Springer Nature. All rights reserved.

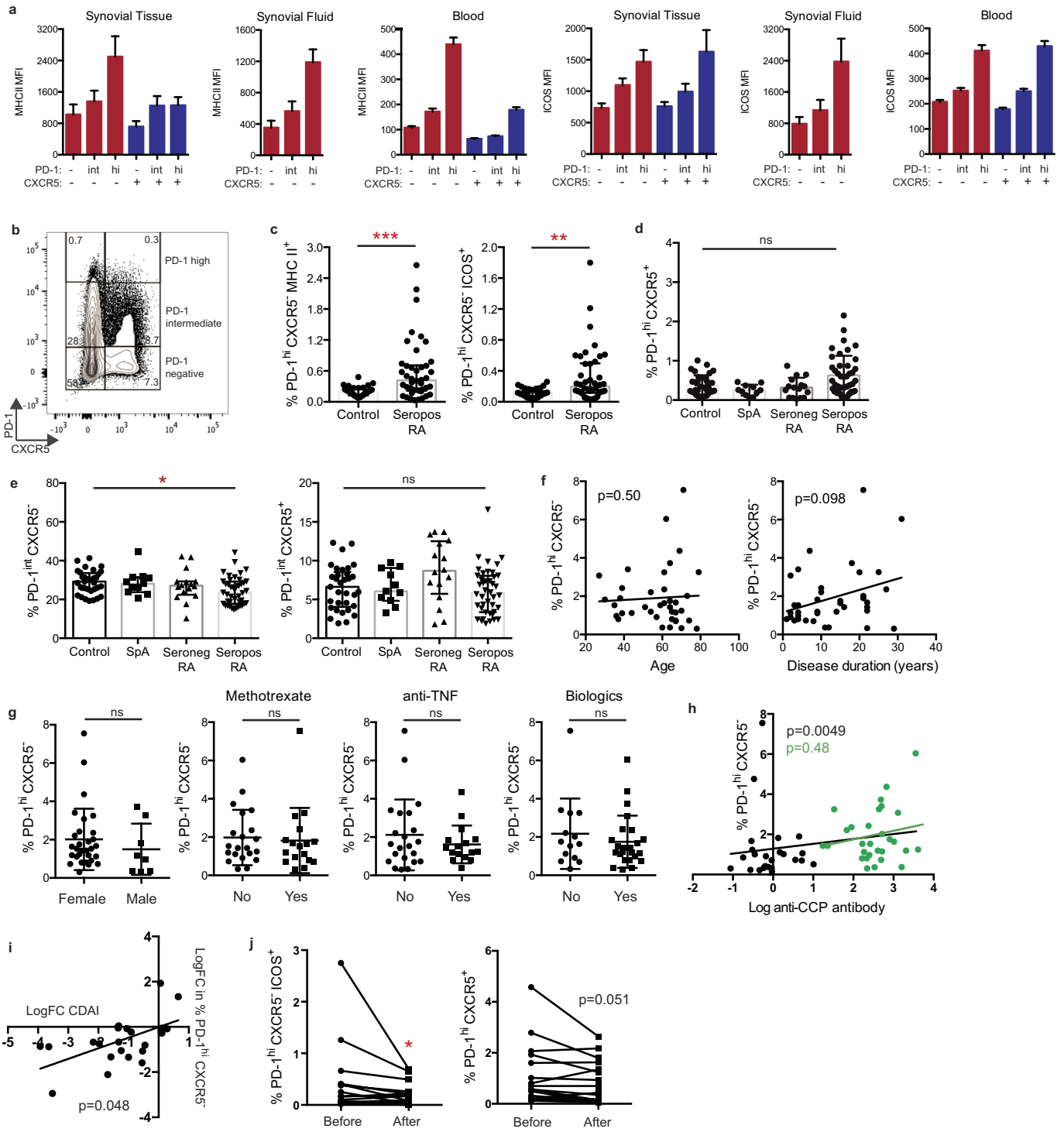

Extended Data Figure 2 | PD-1^{hi}CXCR5^{-}CD4^{+} T cells are expanded in circulation of patients with active, seropositive RA and decrease with response to therapy. a, Mean expression of MHC II and ICOS in memory CD4^{+} T cell populations from synovial tissue ($n = 10$), synovial fluid ($n = 9$), and blood ($n = 42$) from patients with seropositive RA. Mean ± s.d. shown. **b**, Flow cytometric detection of PD-1 and CXCR5 expression on blood memory CD4^{+} T cells. **c–e**, Frequency of PD-1^{hi} cells that co-express MHC II or ICOS (**c**), PD-1^{hi} CXCR5^{+} cells (**d**) or cells with intermediate PD-1 expression (**e**) within memory CD4^{+} T cells from blood of patients with seropositive RA ($n = 42$), seronegative RA ($n = 16$), spondyloarthropathy (SpA, $n = 11$), and non-inflammatory controls ($n = 35$). **f**, Correlation between age or disease duration and blood PD-1^{hi}CXCR5^{-} cell frequency in seropositive RA patients ($n = 38$). **g**, PD-1^{hi}CXCR5^{-} cell frequencies in seropositive RA patients segregated based on sex or medication usage ($n = 38$). **h**, Correlation between serum anti-CCP antibody titer and blood PD-1^{hi}CXCR5^{-} cell frequency in all RA patients ($n = 53$, black line, $P = 0.0049$) or in only anti-CCP antibody^{+} patients ($n = 29$, green line, $P = 0.48$). **i**, Correlation between fold change in CDAI and fold change in PD-1^{hi}CXCR5^{-} cell frequency in patients 3 months after addition of a new RA medication ($n = 23$; methotrexate, 11; anti-TNF, 4; abatacept, 4; tocilizumab, 2; tofacitinib, 2). **j**, Frequency of PD-1^{hi} T-cell subpopulations in blood before and after RA treatment escalation in 18 patients with reduced disease activity after therapy. Median ± interquartile range (**c–e**); mean ± s.d. (**a, g**) shown. $^{*}P < 0.05$, $^{**}P < 0.01$, $^{***}P < 0.001$, $^{****}P < 0.0001$ by Mann–Whitney (**c, g**), Kruskal–Wallis (**d, e**), Wilcoxon test (**j**). In **f, h, i**, P values calculated by Spearman correlation.

© 2017 Macmillan Publishers Limited, part of Springer Nature. All rights reserved.

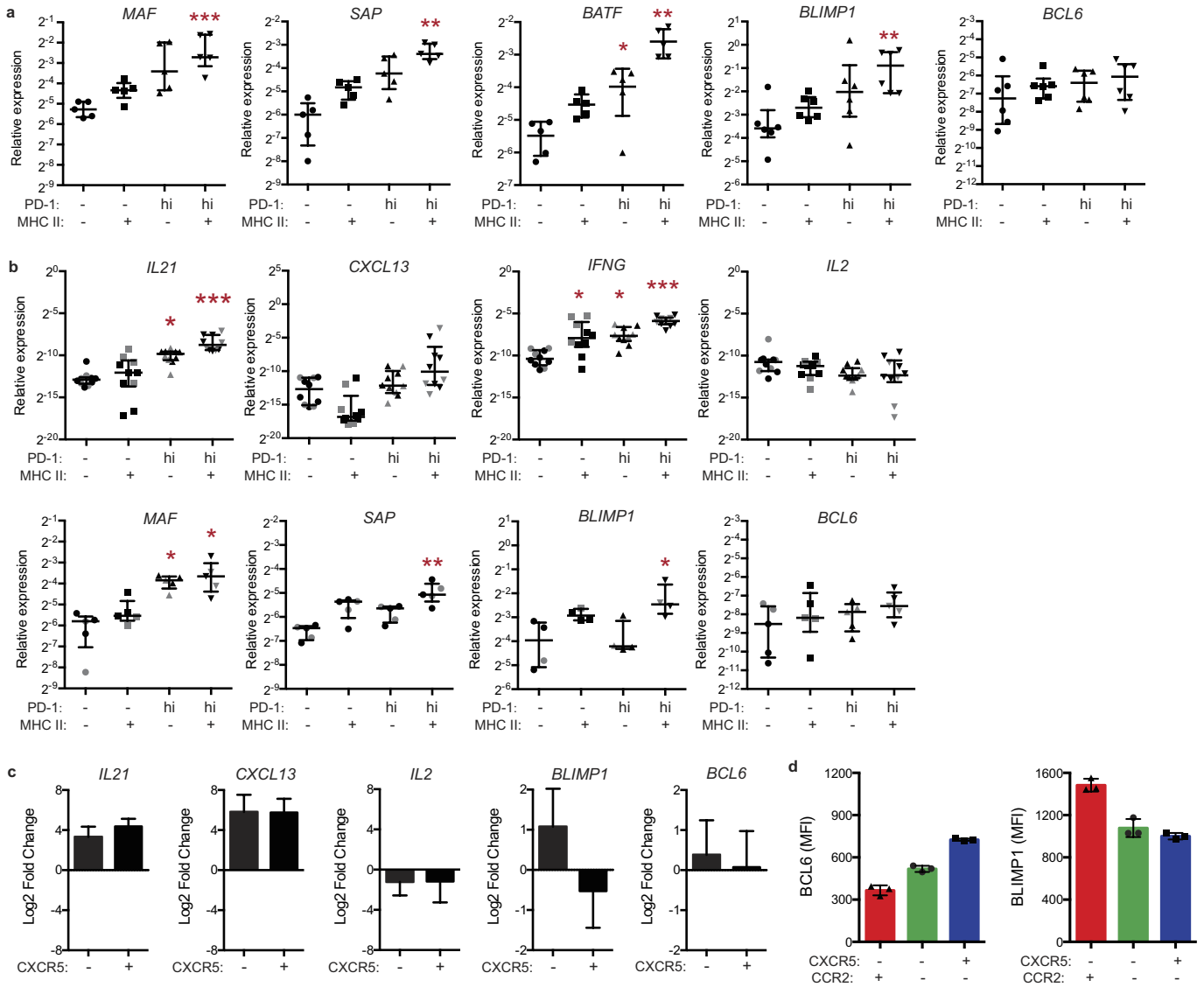

Extended Data Figure 3 | Blood PD-1^{hi}CXCR5^{-}CD4^{+} T cells express factors associated with B-cell help. a, RT–PCR for intracellular regulators in memory CD4^{+} T cell populations from RA synovial fluid ($n = 5$ or 6 donors). **b**, RT–PCR for cytokines ($n = 10$ donors, 6 RA patients (black), 4 controls (grey)) and intracellular regulators ($n = 4$ or 5 donors) in memory CD4^{+} T cell populations from blood. **c**, Cytokine and transcription factor mRNA expression in blood PD-1^{hi} memory CD4^{+} T cell populations divided according to CXCR5 expression, relative to PD-1^{-} cells ($n = 6$ donors). **d**, Flow cytometric quantification of BCL6 and BLIMP1 in blood PD-1^{hi} memory CD4^{+} T cell subpopulations sorted according to chemokine receptor expression, then stimulated *in vitro* for 2 days with anti-CD3/CD28 beads. Representative data from 1 of 3 experiments using cells from different donors. Median ± interquartile range (**a**, **b**); mean ± s.d. (**c**, **d**) shown. *$P < 0.05$, **$P < 0.01$, ***$P < 0.001$ by Friedman's test, compared to PD-1^{-}MHC-II^{-} group (**a**, **b**).

© 2017 Macmillan Publishers Limited, part of Springer Nature. All rights reserved.

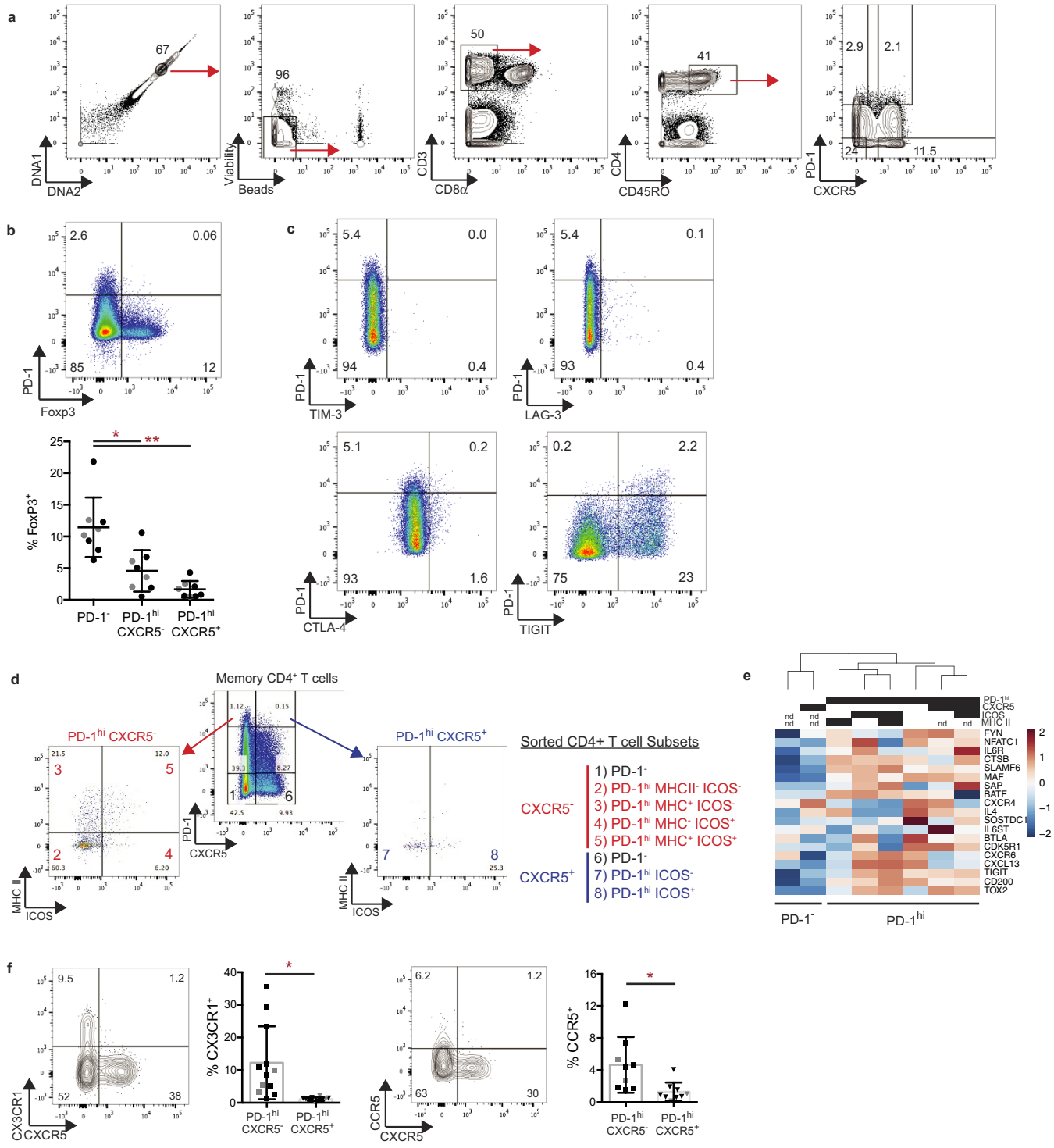

Extended Data Figure 4 | Identification and characterization of circulating PD-1^{hi}CXCR5^{-} and PD-1^{hi}CXCR5^{+} in mass cytometry and RNA-seq analyses. a, Gating of blood PD-1^{hi} memory CD4^{+} T cells in mass cytometry analyses. **b**, Flow cytometric detection of FOXP3 and PD-1 in blood memory CD4^{+} T cells from patients with RA (black, $n = 5$) and controls (grey, $n = 3$). **c**, Flow cytometric detection of inhibitory receptors on blood CXCR5^{-} memory CD4^{+} T cells. Data from 1 of 3 patients with RA with similar results. **d**, Sorting strategy for PD-1^{hi}CXCR5^{-} and PD-1^{hi}CXCR5^{+} cell populations for RNA-seq. **e**, Hierarchical clustering T-cell subpopulations sorted as in **d**, with clustering based on expression of T_{FH}-associated genes measured by RNA-seq. **f**, Chemokine receptor expression on blood memory CD4^{+} T cells from patients with RA (black) or controls (grey) by flow cytometry. Mean ± s.d. shown. *$P < 0.05$, **$P < 0.001$, ***$P < 0.0001$ by Kruskal–Wallis test compared to PD-1^{-} cells (**b**) or Wilcoxon test (**f**).

© 2017 Macmillan Publishers Limited, part of Springer Nature. All rights reserved.

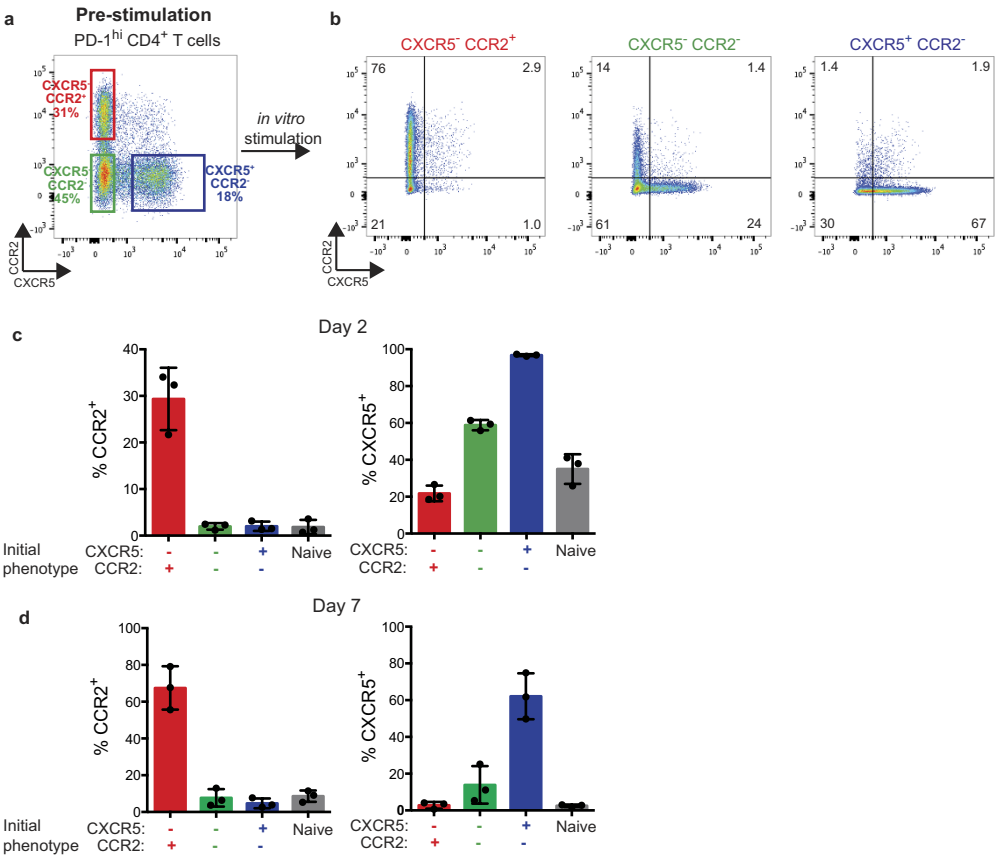

Extended Data Figure 5 | Limited interconversion of PD-1^{hi}CCR2^{+} and PD-1^{hi}CXCR5^{+} T cells *in vitro*. **a**, Flow cytometry of CXCR5 and CCR2 on gated PD-1^{hi} memory CD4^{+} T cells from blood. **b**, Expression of CXCR5 and CCR2 on indicated sorted PD-1^{hi} T-cell populations 7 days after *in vitro* stimulation with anti-CD3/CD28 beads. **c**, **d**, Percentage of cells from each sorted PD-1^{hi} population that expressed CXCR5 or CCR2 on day 2 (**c**) or day 7 (**d**) after *in vitro* stimulation. Naive CD4^{+} T cells are shown as control. Mean ± s.d. shown ($n = 3$ donors from 3 separate experiments).

© 2017 Macmillan Publishers Limited, part of Springer Nature. All rights reserved.

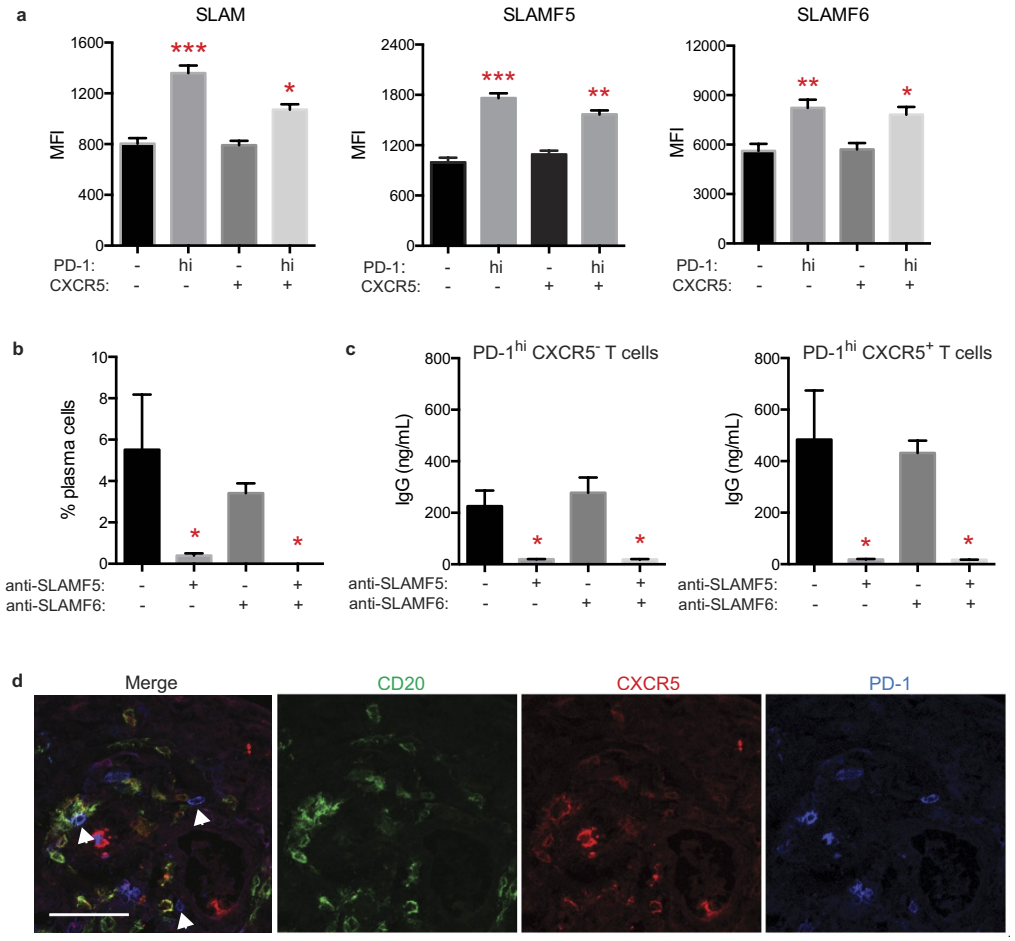

Extended Data Figure 6 | SLAMF5 is required for B-cell-helper function of PD-1^{hi}CXCR5^{-}CD4^{+} T cells. a, Flow cytometric quantification of SLAM, SLAMF5, and SLAMF6 expression on memory CD4^{+} T cells ($n = 10$ donors; 5 patients with RA, 5 controls). **b**, Quantification of frequency of memory B cells with plasma cell markers after co-culture with PD-1^{hi}CXCR5^{+}CD4^{+} T cells with addition of blocking antibodies against SLAMF5 and/or SLAMF6. **c**, IgG quantification by ELISA in co-cultures of memory B cells with PD-1^{hi}CXCR5^{-} or PD-1^{hi}CXCR5^{+} T cells with addition of blocking antibodies against SLAMF5 and/or SLAMF6. For **b**, **c**, 1 of 3 experiments with similar results ($n = 3$ replicates shown). Mean ± s.d. shown. $^{*}P < 0.05$, $^{**}P < 0.01$, $^{***}P < 0.001$ by Kruskal–Wallis compared to PD-1^{-}CXCR5^{-} (**a**) or isotype control (**b**, **c**). **d**, Immunofluorescence microscopy of CD20 (green), CXCR5 (red), and PD-1 (blue), in seropositive RA synovial tissue. Arrows point to PD-1^{hi}CXCR5^{-} cells adjacent to B cells. Scale bar, 50 μm.

© 2017 Macmillan Publishers Limited, part of Springer Nature. All rights reserved.

Extended Data Table 1 | Mass cytometry panels for analysis of synovial and blood cells

	Synovial Panel		Blood Cell Panel	
Metal	**Target**	**Clone**	**Target**	**Clone**
89Y	CD45	HI30		
103Rh			Live/Dead	Cell-ID
141Pr	CD27	M-T271	CD27	M-T271
142Nd	CD19	HIB19	CD45RA	HI100
143Nd	RANKL	MIH24	CD44	BJ18
144Nd	CD64	10.1	CD39	A1
145Nd	CD16	3G8	CD16	3G8
146Nd	CD8α	RPA T8	CD8α	RPA T8
147Sm	FAP	Poly	CD45RO	UCHL1
148Nd	CD20	2H7	CD28	CD28.2
149Sm	CD45RO	UCHL1	CD25	M-A251
150Nd	CD38	HIT2		
151Eu	PD-1	EH12.2H7	PD-1	EH12.2H7
152Sm	CD14	M5E2		
153Eu	CD69	FN50	CD69	FN50
154Sm	CXCR5	J252D4	CXCR5	J252D4
155Gd	CD4	RPA T4	CD4	RPA T4
156Gd	Podoplanin	NC-08	CD73	AD2
158Gd	CD3	UCHT1	CD3	UCHT1
159Tb	CD11c	Bu15	CD57	HCD57
160Gd	FcRL4	413D12	ICOS	C398.4A
161Dy	CD138	MI15		
162Dy	CD90	5E 10	CXCR3	G025H7
163Dy	CCR2	K036C2		
164Dy	Cadherin11	23C6	CD161	HP-3G10
165Ho	FoxP3	PCH101	FoxP3	PCH101
166Er	CD34	581		
167Er	CD146	SHM-57	CD38	HIT2
168Er	IgA	9H9H11	CCR6	G034E3
169Tm	TCRgd	B1	CCR7	G043H7
170Er	ICOS	C398.4A		
171Yb	CD66b	G10F5	CD127	A019D5
172Yb	IgM	MHM-88	CD122	TU27
173Yb	CD144	BV9	TIGIT	MBSA43
174Yb	MHCII	L243	HLA-DR	L243
175Lu	IgD	IA6-2	Tbet	4B10
176Yb	VCAM-1	STA	Perforin	dG9
195Pt	Live/Dead	Cell-ID		

© 2017 Macmillan Publishers Limited, part of Springer Nature. All rights reserved.

Extended Data Table 2 | Clinical characteristics of evaluated patients

	Patient	#1	#2	#3	#4	#5	#6	#7	#8	#9	#10
Synovial Tissue Donors	Age	57	54	76	46	46	79	62	63	52	43
	Sex	F	F	F	F	F	F	M	M	F	F
	Disease Duration (years)	13	17	4	8	19	0.5	19	8	N/A	N/A
	CDAI	14	9	17	15	21	25	5	9	N/A	N/A
	CRP (mg/L)	25	8	8	11	17	19	13	66	76	0.8
	Methotrexate	No	Yes	No	No	No	No	No	Yes	No	No
	Biologic therapy	Yes	Yes	Yes	Yes	Yes	No	No	No	No	Yes
	Other synthetic DMARD	Yes	No	Yes	No	Yes	No	No	No	Yes	No

		Control	Seropositive RA	Seronegative RA	Spondylo-arthropathy
Blood Cross-sectional cohort	Number	35	42	16	11
	Age	61 ± 13	58 ± 14	58 ± 13	48 ± 12
	Female	22 (63)	33 (78)	11 (69)	5 (45)
	Disease Duration (years)	N/A	13 ± 9	14 ± 10	10 ± 6
	CRP (mg/L)	ND	9.3 ± 17.4	6.3 ± 8.5	3.9 ± 4.2
	CDAI	ND	13.7 ± 8.1	9.8 ± 7.6	ND
	Methotrexate	0	19 (45)	8 (50)	2 (18)
	Anti-TNF	0	16 (38)	6 (38)	10 (90)
	Other biologics	0	10 (24)	5 (31)	0
	Other synthetic DMARD	0	4 (10)	1 (6)	0

		Improved	Not Improved
Blood Longitudinal cohort	Number	18	5
	Age	49 ± 17	57 ± 10
	Female	17 (94)	4 (80)
	CDAI Before	17.6 ± 9.3	21.7 ± 8.9
	CDAI After	6.3 ± 4.2	25.6 ± 10.2
	Started methotrexate	7	4
	Started anti-TNF	4	0
	Started other biologic	7	1

Synovial tissue samples from patients 1–6 were used for mass and flow cytometry phenotyping. Samples from patients 7–10 were also included in flow cytometry phenotyping. Average ± s.d. shown. Parentheses indicate percentage of patients. Other biologics include abatacept, rituximab, tocilizumab, and tofacitinib.

© 2017 Macmillan Publishers Limited, part of Springer Nature. All rights reserved.

Extended Data Table 3 | Significantly differentially expressed genes between PD-1^{-} and PD-1^{hi} cell populations

Gene	logFC PD-1^{neg} vs PD-1^{hi}	p-value	adjusted p-value
PD-1	-6.39	1.03E-17	2.07E-13
TOX	-3.97	7.21E-13	7.21E-09
ITM2A	-1.21	4.54E-10	3.02E-06
TIGIT	-1.92	1.03E-09	5.15E-06
MAF	-1.42	4.43E-09	1.77E-05
CA6	3.05	6.13E-09	2.04E-05
CST7	-3.16	1.47E-08	3.80E-05
SCML1	3.90	1.71E-08	3.80E-05
SCO2	-5.20	1.67E-08	3.80E-05
CDCA7	-4.50	2.56E-08	5.12E-05
RAB37	-1.57	6.90E-08	1.15E-04
ICA1	-2.95	2.32E-07	3.24E-04
EZH2	-3.02	2.43E-07	3.24E-04
GZMK	-2.75	2.68E-07	3.35E-04
MAP3K9	-2.36	4.44E-07	5.22E-04
PFN1	-1.46	7.05E-07	7.05E-04
SLAMF6	-1.24	8.88E-07	8.18E-04
EPSTI1	-2.04	8.99E-07	8.18E-04
NEFL	4.05	1.14E-06	9.90E-04
CHN1	-3.45	1.22E-06	1.01E-03
UBE2L6	-1.23	1.55E-06	1.14E-03
FANCI	-2.79	1.77E-06	1.26E-03
PSMA4	-1.42	2.22E-06	1.48E-03
TOX2	-3.64	2.72E-06	1.70E-03
FABP5	-2.44	3.07E-06	1.81E-03
ANXA2	-1.27	3.38E-06	1.93E-03
CTLA4	-1.74	4.31E-06	2.33E-03
PLAG1	3.60	4.77E-06	2.51E-03
HVCN1	-3.52	5.08E-06	2.61E-03
FAM210A	-2.78	5.37E-06	2.68E-03
ALOX5	3.44	5.88E-06	2.80E-03
RGS1	-1.20	6.09E-06	2.83E-03
MYL6B	-3.07	8.27E-06	3.65E-03
CEP128	-3.16	8.18E-06	3.65E-03
ENC1	-3.61	8.40E-06	3.65E-03
MIS18BP1	-2.07	8.89E-06	3.78E-03
F5	-1.46	1.00E-05	4.05E-03
FN1	2.50	1.07E-05	4.05E-03
CXCR3	-3.02	1.06E-05	4.05E-03
ASB13	3.35	1.06E-05	4.05E-03
HIST2H2BF	3.68	9.85E-06	4.05E-03
PRR5L	-2.17	1.10E-05	4.08E-03
KRT72	3.19	1.24E-05	4.43E-03
BZRAP1	-1.97	1.37E-05	4.81E-03
DUSP2	-1.46	1.55E-05	5.33E-03
DHFR	-2.73	1.74E-05	5.62E-03
FBXO41	-2.41	1.94E-05	6.14E-03
CCDC86	-3.43	1.99E-05	6.21E-03
FCRL3	-1.77	2.06E-05	6.27E-03
AKR1C3	-3.31	2.07E-05	6.27E-03
SHMT2	-1.53	2.17E-05	6.38E-03
DDX54	-1.73	2.21E-05	6.41E-03
UBE2A	-1.32	2.88E-05	7.68E-03
ANXA9	2.92	2.85E-05	7.68E-03
TUBB4B	-1.24	3.12E-05	8.10E-03
TIMELESS	-2.61	3.24E-05	8.26E-03
CCL5	-3.36	3.26E-05	8.26E-03
UQCRC1	-1.29	3.42E-05	8.44E-03
TBC1D4	-1.30	3.49E-05	8.51E-03
SYT11	-1.38	3.88E-05	9.23E-03
PMAIP1	-2.19	3.84E-05	9.23E-03
DIRC2	-2.78	4.00E-05	9.30E-03
SOX8	1.94	4.26E-05	9.80E-03
SPG20	1.80	4.50E-05	9.90E-03
DPP3	-1.96	4.39E-05	9.90E-03
DUSP4	-2.50	4.50E-05	9.90E-03

© 2017 Macmillan Publishers Limited, part of Springer Nature. All rights reserved.

Extended Data Table 4 | Significantly differentially expressed genes between PD-1^{hi}CXCR5^{-} and PD-1^{hi}CXCR5^{+} cell populations

Gene	logFC PD-1^{hi} CXCR5^{neg} vs PD-1^{hi} CXCR5^{pos}	p-value	adjusted p-value
RPL39	-1.23	1.42E-07	2.30E-04
LSP1	1.20	2.65E-07	2.94E-04
RPL34	-1.27	7.88E-07	4.77E-04
TTC4	4.63	1.29E-06	6.30E-04
LIME1	1.56	2.07E-06	9.20E-04
CCR2	5.09	2.25E-06	9.58E-04
ACTN4	2.32	2.83E-06	1.13E-03
CTSH	2.65	3.19E-06	1.25E-03
PLAC8	-1.35	6.85E-06	2.36E-03
GLIPR2	1.40	7.14E-06	2.38E-03
PRR5	2.82	1.02E-05	3.06E-03
RGS19	2.46	1.19E-05	3.45E-03
SAMD3	1.25	2.50E-05	6.51E-03
FOS	-1.60	3.68E-05	8.77E-03
ANXA4	2.27	4.03E-05	9.37E-03
LTK	3.89	4.20E-05	9.66E-03

© 2017 Macmillan Publishers Limited, part of Springer Nature. All rights reserved.